

IMPROVEMENT OF A PWR TRANSPORT CORE CALCULATION USING A TWO-LEVEL MODELING TO GENERATE THE HOMOGENEOUS CROSS SECTIONS LIBRARIES.

Anne NICOLAS, Stéphane MENGELLE and Philippe LAFARGE
DRN/DMT/SERMA/LENR
CEN Saclay
91191 Gif sur Yvette cedex
FRANCE

anne.nicolas@cea.fr ; stephane.mengelle@ cea.fr

ABSTRACT

To improve drastically rod calculations in PWR cores, we suggest to calculate the complete 3D core with an improved SPN transport method.

Without discontinuity factors or adjustment, the usual diffusion calculations led to a 10% overestimation of the calculated black rod worth versus measurement. SPN transport calculations gave a 6% overestimation.

Our paper shows a new way to remove partially this residual overestimation. Comparisons with SN calculations showed that the SPN scheme was converged, so the main reason of the residual overestimation are the homogeneous cross sections used in the core calculation.

To get more accurate homogeneous cross sections, we develop a new calculation scheme in the lattice code APOLLO2. The main idea of this method is to combine P_{ij} and SN calculations to take accurately into account the strong flux gradient that occurs in assemblies with black control rods and the stronger flux anisotropy found in such assemblies.

We validate this new methodology both with comparisons to references and measurement when available. The calculated core was a 900 MWe PWR reactor recycling plutonium. The start-up core has been calculated with the usual method (one level scheme to generate cross sections and further 2 groups diffusion calculation) and with the new calculation scheme (two level method to generate cross sections, SP3 P1 3D 8 groups homogeneous transport core calculation). When we use the new methodology to generate the homogeneous cross sections, the residual overestimation of the various control rod banks is still reduced. So, it becomes no more than 4% for homogeneous transport calculations.

1. INTRODUCTION

In previous work, we suggested to use a SP3 transport 3D core calculation to improve the rod worth [1], [2]. The SPN method was chosen, used in the CRONOS2 computer code [3].

Without discontinuity factors or any adjustment, it is well-known that the usual diffusion calculation led to a 10% overestimation of the calculated black rod worth versus measurement in most cases. With the transport calculation, the residual error was a 5% overestimation.

Our paper gives a new way to partially remove this residual overestimation. It has been shown in [4] by comparison with SN calculations that our SPN scheme is converged ; so one of the reasons of the residual overestimation could be the homogeneous cross sections used in the core calculation. To get more accurate ones, we develop a new calculation scheme in the lattice code APOLLO2 [5].

The main idea of this method is to take accurately into account the flux gradient and the flux anisotropy that occur in black rodded assemblies.

Here we develop in the first part the calculation methodology used to generate the homogeneous cross sections for the rodded assemblies, and add some convergence studies to explain our choices ; in the second part, we give the results obtained by the new method for a PWR core recycling plutonium calculation, with a comparison to measurements. Figure 1 describes the assembly geometries and figure 2 is devoted to the core description.

2. METHODOLOGY USED TO GENERATE THE HOMOGENEOUS CROSS SECTIONS

The sequence of calculations used to calculate and homogenize the cross sections is as follows :

1. The first level is devoted to the self-shielding calculations. Self-shielding can be considered as a local phenomena. It is necessary to use an accurate modeling (6 rings in the fuel pin to take into account the rim effect), but a multicell calculation is precise enough to describe the spatial flux. A 172 energy groups mesh is used for both UOX and MOX assemblies.
2. The second level is devoted to the flux gradient and anisotropy calculation, taking into account the first step cross sections, and using a SN flux calculation in the assembly, after an homogenization and condensation stage. We use here a reduced energy mesh (from 8 to 26 groups). All energy meshes used are given in figure 3.. A good agreement of SN calculations with pin-by-pin power was detailed in [6].

Such a method was previously used for BWR assembly calculations [7], and comparisons with Monte-Carlo calculations showed a very good agreement.

The first level is usually used to generate directly homogeneous cross sections. The results are good enough if the calculated assemblies do not contain control rods, but show discrepancies for rodded ones.

A comparison between the power shapes of the first and the second level is shown in figure 4. The reactivity gap is always less than 60 pcm. We compared them for UOX and MOX assemblies, with and without control rods. We can notice that the more the assembly is heterogeneous, the more the two level calculation is necessary. The increasing heterogeneity is : unrodded UOX,

unrodded MOX, rodded MOX, rodded UOX (this comes from the stronger efficiency of the absorber in the UOX assembly and from the three enrichment zones of the MOX assemblies).

2.1 FIRST LEVEL : SELF-SHIELDING CALCULATION.

The calculation scheme is a 172 energy group multicell assembly calculation, in infinite medium, using the collision probability method (Pij) coupled by interface currents. It has been shown that this representation is accurate enough for assemblies without strong heterogeneity.

The library mainly comes from the JEF 2 evaluation, and the 172 energy group mesh is the standard library for APOLLO2.

The self shielding modeling used is detailed in [8].

After the self-shielding calculation, it is necessary to transmit cross sections to the “second level”. They have to be homogenized and condensed to get a low cost SN. To get a good result, it is necessary to apply an equivalence procedure in order to keep the precise reference calculation reaction rates in a Pij calculation.

The cross sections are condensed on a 26 groups mesh, over the reference geometry flux, optimized for this kind of calculation, and are given by :

$$\sigma = \frac{\int_G \sigma(E)\Phi(E)dE}{\int_G \Phi(E)dE}$$

The homogenized cross sections are given by :

$$\Sigma_M = \frac{\sum_{m \in M} \Sigma_m V_m \Phi_m}{\sum_{m \in M} V_m \Phi_m}$$

M is the macroregion containing the microregions m. In this scheme, microregions are fuel, clad, moderator, absorber ... and we keep one macroregion per cell (consequently, 269 macroregions per assembly and 45 because of the 1/8 symmetry).

Both simplifications (homogenization and condensation) need to use an equivalence process, in which the first level reference reaction rates are kept.

Some studies have been done, to determine the best way to compute the equivalence factors, reducing to the maximum the time in the first level. The convergence criteria here given is the gap between two equivalence coefficients in two successive iterations. It determines the iteration number, and consequently the first level calculation time. The sensitivity of this criteria is given in the next table, for a black rodded assembly.

Criteria	k_{inf}	gap (pcm)	Iteration number	Time (s)
10^{-5}	0.81496	Reference	346	127
$5 \cdot 10^{-5}$	0.81496	0	199	87
10^{-4}	0.81496	0	135	66
10^{-3}	0.81495	1	15	32
10^{-2}	0.81426	86	5	27

Table 1 : Equivalence convergence criteria effect (first level, 26 energy groups)

From this results, we choose to use a 10^{-4} criteria.

At this step, we have a cross section library, homogenized and condensed for the second level.

2.2 SECOND LEVEL : SN FLUX CALCULATION.

To increase the rodded assemblies calculation accuracy, an interesting way is to compute them with a discrete ordinates method. It allows a good treatment of flux anisotropy and flux gradient. Various calculation options have been studied for this part of the calculation scheme :

1. the energy mesh,
2. the spatial mesh,
3. the anisotropy order,
4. the angular representation.

Influence of the condensation mesh.

We compute four different condensation meshes, from 8 to 26 energy groups. They are described figure 3. The 26 groups energy mesh is considered as a reference. The given time is spent in the SN flux calculation. The SN calculation and the spatial mesh are considered as reference ones (S16P5 calculation, 25 meshes per fuel cell). We can notice in those results a little gap on the reactivity (fewer than 50 pcm). In an industrial calculation scheme, we probably had choose a fewer group mesh ; in our study, we choose the reference mesh (26 groups) to compute our homogeneous libraries.

Number of groups	k_{inf}	gap (pcm)	time (s)
26	0.82187	Reference	10137
21	0.82185	2	8349
16	0.82196	11	4484
8	0.82227	48	3244

Table 2 : Influence of the energetical mesh.

Influence of the spatial meshing

Here is realized a convergence study which depends on the meshing of the homogenized fuel or absorber cell, from M1 (one mesh per cell) to M6 (36 - 6X6 - meshes per cell).

We use a S16P5 calculation, using a nodal method (linear flux in the mesh and at the boundary), with 26 energy groups.

mesh	kinf	gap (pcm)	gap MN-MN-1 (pcm)	time (s)
M6	0.82188	reference	reference	14195
M5	0.82187	1	1	10137
M4	0.82184	5	3	6546
M3	0.82177	13	7	3760
M2	0.82151	45	31	1954
M1	0.81984	249	203	838

Table 3 : Influence of the spatial meshing

The power shape criteria shows that a M1 mesh is not precise enough ; the absorption rate is underestimated by 0.7% to 0.9% in the absorber cell. A M4 mesh induces a gap of 5 pcm with the reference, and a gap for reaction rates less than 0.02%. So, we choose the M4 mesh to compute our homogeneous libraries.

The nodal linear approximation is more expensive than the usual diamond scheme, but its convergence is faster.

Influence of the anisotropy order.

Here is described the convergence of the reactivity from an order 0 to an order 5 for the Legendre polynomials cross sections development.

Anisotropy order	kinf	gap (pcm)	gap PN-PN-1 (pcm)	time (s)
P5	0.82187	reference	reference	14195
P4	0.82187	0	0	8387
P3	0.82188	1	1	7284
P2	0.82198	13	12	6680
P1	0.82054	162	175	6094
P0*	0.82459	330	492	4250

P0* : P0 order with a transport correction (used for the Pij calculation scheme).

Table 4 : Influence of the anisotropy order.

We notice in those results that a P3 development is accurate enough to represent black rodged assemblies flux anisotropy.

Influence of the angular representation.

We compute calculations from S4 to S32. Results are given in table 5.

direction number	k _{inf}	gap (pcm)	gap SN-SN-1 (pcm)	time (s)
S32	0.82196	reference		37931
S24	0.82197	1	1	21327
S16	0.82187	11	12	10137
S12	0.82169	33	22	6000
S8	0.82143	64	32	2995
S4	0.82081	140	75	1018

Table 5 : Influence of the angular representation.

Looking to the k_{INF} values, we choose S16 calculations to compute reference libraries. Moreover, we verify that the maximum reaction rates gap is always under 0.03%.

Finally, the chosen options to compute homogeneous reference libraries are :

1. a 26 energy group mesh
2. a S16 P3 SN calculation, 16 meshes per cell.
3. a 10^{-4} convergence criteria in the equivalence process.

3. VALIDATION : ROD WORTH CALCULATION FOR A 900 MWe PWR.

In previous work [1] we showed that a SPN transport core calculation could improve the control rod worth calculation : the discrepancy between calculation and measurement was reduced by half for most of the rods. Using our new homogenization method, we still reduce the residual discrepancy.

We have opted to present the results obtained for a 900 MWe reactor recycling plutonium. One third of the fuel assemblies in this reactor are of the MOX type for an equilibrium cycle. The results are shown on the previous cycle (with only two batches of MOX assembly). This reactor core contains two types of MOX assemblies and two types of UOX assemblies. The core is described in figure 2 (rods and different fuel assemblies positions).

The cycle described in our results uses an initial burn-up plan with a 3 batch loading. A quarter core with the three different batches is represented in fig. 5.

Previous studies [4] made possible to identify the options required for a SPN core transport calculation. They showed the necessity to use the SP3 for the homogeneous cases. The comparisons between simplified transport (SPN) and exact transport (SN) [3] [4], showed the good agreement between this two methods. For comparison purposes, we also carried out the two group diffusion calculation using the same libraries.

The CRONOS2 calculations are characterized as follows :

- 3D SP3_P1 complete core calculation.
- Use of the Minos solver (mixte dual method) [3].
- 2nd degree polynomials in the X, Y and Z directions (homogeneous).

- Exact integration along the X, Y and Z axes.
- Spatial meshing is described in table 6.

Mixed finite element method Simplified transport SP3 P1 with 8 energy groups			
Axis	X	Y	Z
Number of meshes	17	17	23
Calculation point by mesh	2	2	1
Polynomial degree	2	2	2

Table 6 Spatial meshing.

This represents 7 million flux calculation points and 21 million current calculation points for the whole core.

Reflector constants have been generated by the method developed in [1].

Table 7 shows various control rod worth calculations. We compare 2 group diffusion (one-level library) calculations to 8 groups SP3_P1 transport ones (one-level and two-level libraries).

rod	2 groups diffusion / measurement (one level library)	8 groups SP3_P1 / measurement (one level library)	8 groups SP3_P1 / measurement (two level library)	8 groups SP3_P1 one level library / two level library
R	+10.0 %	+4.9 %	+2.6 %	-2.3 %
G1	+6.2 %	+4.0 %	+1.9 %	-2.1 %
G2	+7.1 %	+5.7 %	+3.6 %	-2.1 %
N1	+8.2 %	+3.6 %	+1.8 %	-1.8 %
N2	+2.6 %	+4.7 %	+3.7 %	-1.0 %

Table 7 : Rod worth calculations : discrepancies

We notice an improvement of the rod worth calculation, getting at least a 4% maximum overestimation with the new calculation scheme.

CONCLUSION

In previous work, to improve the rod worth calculations, we suggested to use a SP3 transport core calculation. With this approach, the discrepancy between measurement and calculation was reduced by half. To improve these results, we propose to use a new method to generate the homogeneous cross sections for to the core calculation. The main idea of the new calculation scheme is to separate in two steps the assembly calculations : the first one is devoted to the self-shielding calculation, using a Pij approximation for the flux calculation ; the second stage, is devoted to the flux gradient calculation, using a discrete ordinate method. This allows to take correctly into account the flux gradient and anisotropy in the rodded assemblies.

When the homogenized cross sections obtained by this method are used to compute a PWR 900 MWe start up measurements, the residual overestimation of the control rod worth is still reduced,

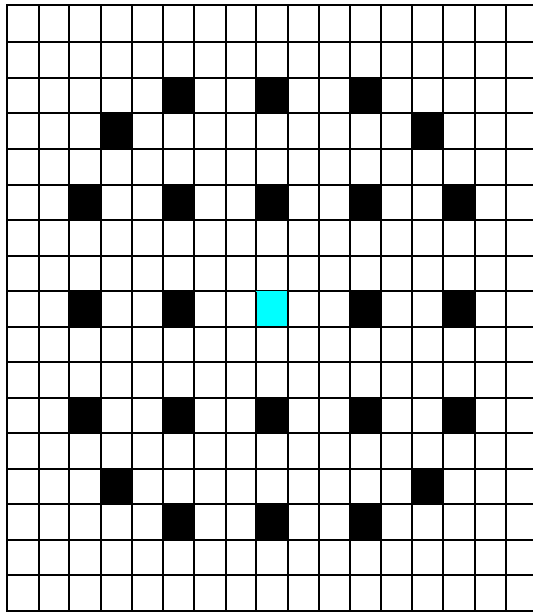
and is always less than 4%.. These promising results have to be confirmed for other core calculations.

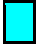


In order to improve the calculation time and accuracy, the next stage of this work, dedicated to develop a new calculation scheme for power reactors based on transport core calculations, is to optimize both the core calculation (energy meshing, choice of the simplified transport) and the stage devoted to generate the homogeneous cross sections.

REFERENCES

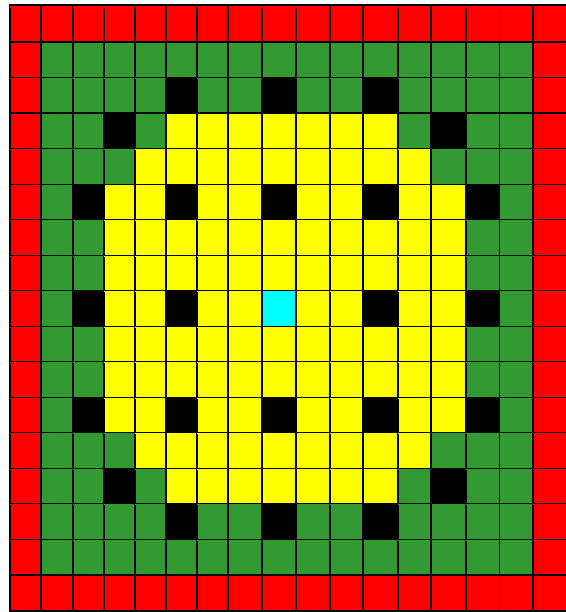
1. E. Richebois, S. Mengelle, A. Nicolas et al. "Determination of Multigroup and Multioperator Reflector Constants. Application to a Power Reactor Calculation", Proceedings of International Conference on the Physics of Nuclear Science and Technology, Long Island, New York, Vol. 1, pp. 1018-1028, (1998).
2. S. Mengelle, A. Nicolas et al. "A New Power Reactor 3D Transport Calculation Scheme using the CRONOS2 and APOLLO2 Codes" Proceedings of Mathematics and Computation, Reactor Physics and Environmental Analysis in Nuclear Applications, Madrid, Vol. 2, pp. 1047-1054, (September 1999).
3. C. Fedon-Magnaud et al. "Pin-by-pin Transport Calculation with the CRONOS2 Reactor Code" Proceedings of Mathematics and Computation, Reactor Physics and Environmental Analysis in Nuclear Applications, Madrid, Vol. 2, pp. 1278-1287, (September 1999).
4. E. Richebois, « Calcul de cœur REP en transport 3D » PhD Thesis, Université de Marseille Provence, Mai 1999.
5. S. Loubière et al. "APOLLO2 twelve years later," Proceedings of Mathematics and Computation, Reactor Physics and Environmental Analysis in Nuclear Applications, Madrid, Vol. 2, pp. 1298-1318, (September 1999).
6. P. Blanc-Tranchant et al., "Definition and validation of a 2D Transport scheme for PWR Control Rod Clusters" Proceedings of Mathematics and Computation, Reactor Physics and Environmental Analysis in Nuclear Applications, Madrid, Vol. 2, pp. 1074-1085, (September 1999).
7. F. Bouveret, "Two Level Flux Calculation System for Producing Multi-Parameter Libraries using APOLLO2 for a Dodewaard Fuel Assembly" Proceedings of Mathematics and Computation, Reactor Physics and Environmental Analysis in Nuclear Applications, Madrid, Vol. 1, pp. 901-907, (September 1999).
8. M. Coste et al., « Self-shielding calculation by APOLLO2 code for fuel pins with a temperature distribution. » Joint International Conference on Mathematical Methods and Supercomputing in Nuclear Applications, Vol. 1, pp. 446-455, Saratoga Springs, New York, USA (1997)

UOX assembly



-  water hole
-  absorber
-  fuel

MOX assembly



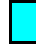




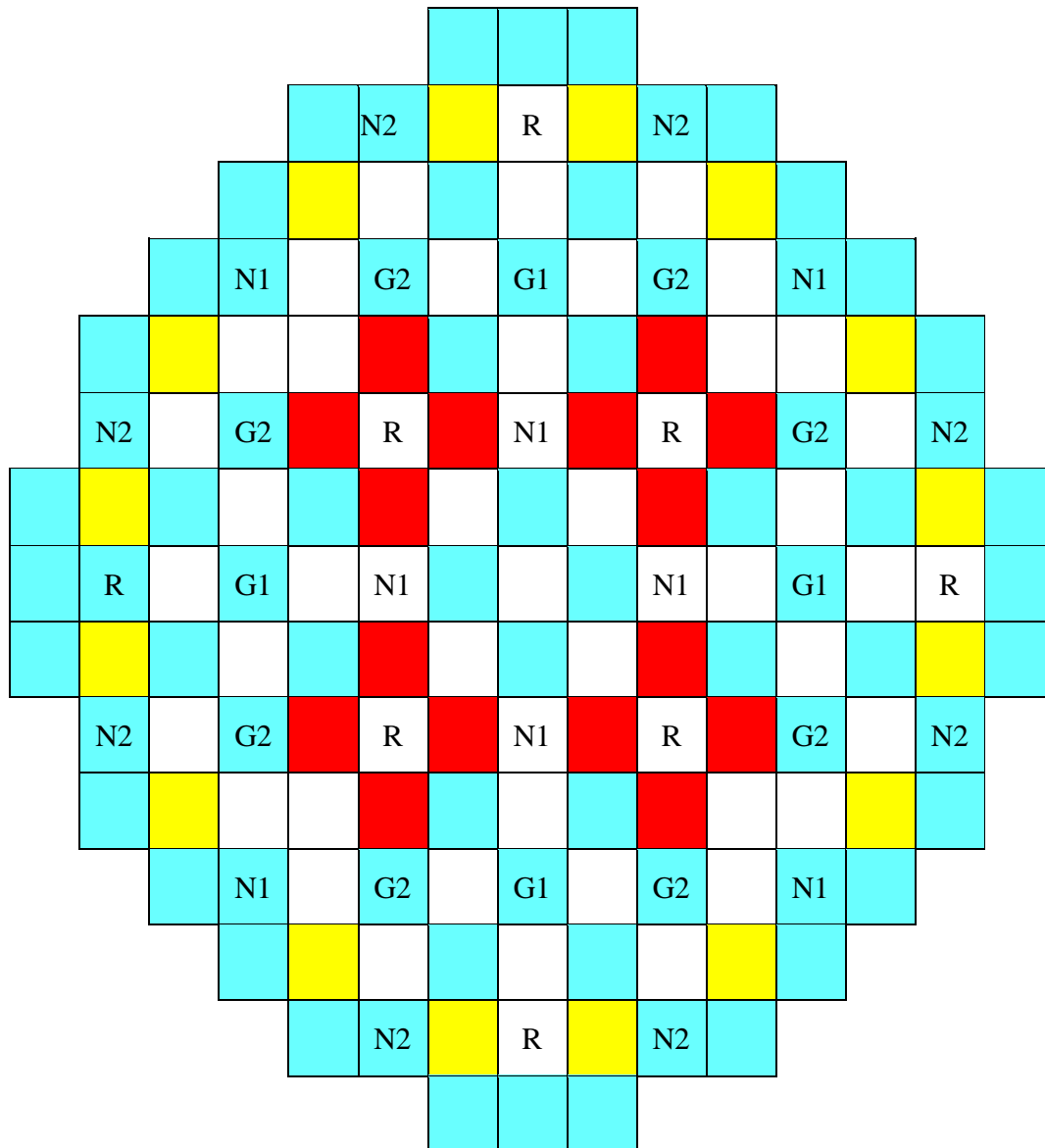
-  water hole
-  absorber
-  fuel 1 (lower enrichment)
-  fuel 2 (middle enrichment)
-  fuel 3 (higher enrichment)

Figure 1. Fuel assemblies contained in the calculated core



MOX 1



MOX 2



UOX 1



UOX 2

R ; N1 ; N2 : black rods – G1 ; G2 : grey rods

Figure 2. Control rod position in a 900 MWe PWR.

Limit in energy (MeV)	Meshes used in the second level			Meshes used in the core calculation	
	26 groups	21 groups	16 groups	8 groups	2 groups
20	1	1	1	1	1
5.4881	2	2	2		
2.0190	3	3	3		
1.3534	4		4		
9.0718 10-1	5	4		2	
4.0762 10-1	6		5		
2.7323 10-1	7	5		3	
1.8316 10-1	8	6	6		
5.5166 10-2	9	7	7		
2.4788 10-2	10	8	8		
7.4659 10-3	11		9		
5.0045 10-3	12	9		4	
2.2487 10-3	13	10	10		
4.5400 10-4	14	11	11		
2.4981 10-5	15	12	12		
4.1293 10-6	16	13	13		
2.7679 10-6	17	14	14	5	
1.6700 10-6	18	15		6	
6.2500 10-7	19	16		7	2
5.4001 10-7	20		15		
2.2000 10-7	21	17			
1.6000 10-7	22	18		8	
9.5000 10-8	23		16		
7.7000 10-8	24	19			
3.0000 10-8	25	20			
1.0000 10-8	26	21			

Figure 3. Energy meshes.

								1,121			
								1,122			
								-0,02			
							1,107	1,113			
							1,101	1,110			
							0,55	0,28			
						1,127	1,111	1,112			
						1,126	1,105	1,107			
						0,11	0,58	0,42			
							1,168	1,125	1,118		
							1,171	1,119	1,113		
							-0,23	0,49	0,42		
					1,171	1,192	1,181	1,138	1,126		
					1,180	1,203	1,190	1,139	1,122		
					-0,72	-0,91	-0,79	-0,07	0,34		
						1,188	1,190		1,166	1,134	
						1,192	1,194		1,169	1,130	
						-0,32	-0,35		-0,24	0,34	
					1,152	1,182	1,154	1,153	1,176	1,142	1,132
					1,151	1,183	1,154	1,154	1,178	1,142	1,127
					0,09	-0,11	0,00	-0,03	-0,17	-0,01	0,39
		1,151	1,151	1,180	1,152	1,150	1,174	1,141	1,132		
		1,150	1,150	1,181	1,151	1,150	1,176	1,141	1,128		
		0,11	0,11	-0,09	0,05	0,01	-0,14	0,01	0,40		
			1,179	1,179		1,179	1,177		1,165	1,136	
			1,180	1,180		1,180	1,179		1,168	1,132	
			-0,05	-0,07		-0,11	-0,16		-0,19	0,40	

standard deviation : 0.34
maximum discrepancy : 0.91

Legend :

first level (reference)
second level
discrepancy

Figure 4.1. Discrepancies between pin power distributions : UOX without control rods

								1,427
								1,466
								-2,76
							1,346	1,390
							1,372	1,423
							-1,93	-2,37
						1,194	1,286	1,342
						1,192	1,303	1,370
						0,13	-1,36	-2,05
					0,379	1,062	1,215	1,291
					0,367	1,053	1,227	1,316
					3,09	0,88	-0,99	-1,88
				0,971	0,941	1,005	1,159	1,247
				0,939	0,910	0,980	1,156	1,267
				3,35	3,28	2,50	0,29	-1,56
			0,359	0,929	0,932	0,379	1,078	1,207
			0,349	0,912	0,916	0,368	1,076	1,229
			2,79	1,84	1,70	2,77	0,27	-1,80
		1,030	0,950	1,004	1,015	0,992	1,122	1,202
		1,020	0,938	0,990	1,001	0,981	1,119	1,224
		0,94	1,20	1,41	1,40	1,12	0,20	-1,83
	1,117	1,055	0,959	1,011	1,021	0,992	1,117	1,195
	1,135	1,051	0,949	0,998	1,008	0,982	1,115	1,218
	-1,66	0,41	1,03	1,28	1,30	1,05	0,18	-1,89
0,011	1,153	1,016	0,368	0,949	0,957	0,378	1,061	1,182
0,012	1,179	1,013	0,359	0,937	0,945	0,369	1,059	1,206
-4,34	-2,25	0,31	2,44	1,25	1,27	2,51	0,19	-2,02

standard deviation : 1.65
maximum discrepancy : 3.35

first level (reference)
second level
discrepancy

Legend :

Figure 4.2. Discrepancies between pin power distributions : UOX with black control rods.

								0,980						
								0,991						
								-1,16						
							1,179	0,950						
							1,174	0,955						
							0,38	-0,61						
						1,144	1,152	0,933						
						1,140	1,144	0,936						
						0,34	0,74	-0,29						
							1,212	1,160	0,931					
							1,212	1,152	0,934					
							0,04	0,63	-0,31					
						1,283	1,201	1,222	1,176	0,935				
						1,290	1,212	1,234	1,181	0,940				
						-0,54	-0,86	-0,93	-0,47	-0,51				
							1,299	1,342		1,233	0,942			
							1,293	1,337		1,241	0,947			
							0,46	0,40		-0,63	-0,52			
						1,181	1,260	1,205	1,238	1,185	1,171	0,938		
						1,175	1,254	1,196	1,230	1,183	1,177	0,942		
						0,48	0,48	0,69	0,59	0,14	-0,51	-0,51		
						1,173	1,176	1,253	1,196	1,228	1,178	1,168	0,937	
						1,169	1,172	1,248	1,188	1,221	1,177	1,174	0,942	
						0,32	0,39	0,39	0,66	0,56	0,11	-0,56	-0,54	
							1,242	1,245		1,264	1,295		1,223	0,940
							1,240	1,242		1,258	1,289		1,232	0,946
							0,19	0,25		0,50	0,46		-0,74	-0,56

standard deviation : 0.55
maximum discrepancy : 1.16

Legend :	first level (reference)
	second level
	discrepancy

Figure 4.3. Discrepancies between pin power distributions : MOX without control rods.

								1,192
								1,226
								-2,78
							1,392	1,142
							1,409	1,168
							-1,23	-2,22
						1,205	1,312	1,098
						1,195	1,319	1,118
						0,84	-0,55	-1,85
					0,257	1,098	1,252	1,062
					0,253	1,088	1,258	1,082
					1,75	0,93	-0,51	-1,86
				1,120	0,971	1,047	1,206	1,035
				1,093	0,951	1,029	1,205	1,054
				2,40	2,10	1,77	0,10	-1,79
			0,239	1,074	1,098	0,258	1,146	1,013
			0,235	1,060	1,084	0,254	1,149	1,034
			1,56	1,34	1,27	1,57	-0,24	-2,13
		1,122	1,071	1,116	1,150	1,027	1,174	1,007
		1,110	1,060	1,101	1,134	1,018	1,176	1,029
		1,10	1,00	1,35	1,39	0,87	-0,16	-2,18
	1,208	1,143	1,076	1,118	1,150	1,025	1,170	1,003
	1,221	1,134	1,066	1,104	1,135	1,017	1,173	1,026
	-1,16	0,75	0,87	1,25	1,31	0,81	-0,21	-2,25
	1,293	1,121	0,241	1,076	1,100	0,256	1,132	0,998
	1,313	1,115	0,238	1,065	1,088	0,253	1,137	1,021
	-1,51	0,60	1,36	1,03	1,09	1,43	-0,38	-2,39

standard deviation : 1.46
maximum discrepancy : 2.78

Legend :

first level (reference)
second level
discrepancy

Figure 4.4. Discrepancies between pin power distributions : MOX with black control rods.

1	1							
3	1	1	1					
3	2	3	1	1				
2	3	2	3	2	1			
3	2	2	2	3	1	1		
3	2	3	2	2	3	1		
2	3	2	2	3	2	1	1	
3	2	3	3	2	3	3	1	

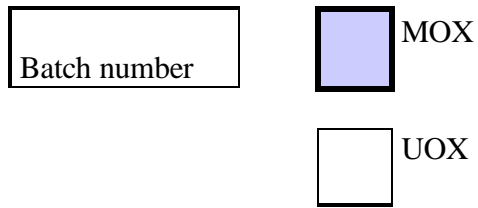


Figure 5. Core burn-up distribution..